Flux Distribution of a Single-Axis Tracking Parabolic Trough Array with Photovoltaic Receiver

G. Burgess and G. Johnston
Centre for Sustainable Energy Systems
Australian National University, Canberra ACT 0200
Australia
E-mail: gregory.burgess@anu.edu.au

Abstract

Single-axis tracking parabolic troughs with photovoltaic cells in series at the receiver require consideration of non-uniformities in the flux distribution. Non-uniformities can result from gaps in mirrors along the length of the trough and from shadowing by receiver support posts. An expression for the flux loss due to a mirror gap is derived, which shows the dependence of the flux distribution on the insolation angle. Photogrammetric analysis and flux mapping demonstrate that the presence of slope errors reduces the magnitude of the non-uniformity.

1. INTRODUCTION

Long arrays of single-axis tracking parabolic troughs with a fluid filled absorber are a well established method of solar power generation. Such a configuration could also be used with photovoltaic cells at the receiver, possibly in combination with a thermal absorber, for direct generation of electrical power. With single-axis tracking the incident solar rays are not in general perpendicular to the trough. Non-uniformity of the flux distribution along the receiver can then occur if there are gaps between reflective surfaces along a trough array, or if there is shadowing by the receiver support structure. Such variations are of relatively little concern for a purely thermal receiver, but where the receiver incorporates a string of series connected photovoltaic cells, regions of low intensity can significantly reduce the overall electrical output.

We first derive the curve on a parabolic trough from which flux is reflected to a given point on the target. This is then used to obtain an expression for the flux which is lost at a photovoltaic cell, due to gaps along an otherwise ideal trough. Imperfections in the reflecting surface, which are determined experimentally using photogrammetry, are shown to reduce the amount of flux loss at the worst cell. Finally, experimental flux maps of a trough with a variable mirror gap are presented.

2. REFLECTIONS FROM AN IDEAL SINGLE-AXIS TROUGH

In the following it is assumed that all incident solar rays are parallel and oriented such that they do not have a component across the width of the trough (x axis in Figure 1). It is always possible to align a single-axis tracking trough so that this is the case, apart from the small angular spread of solar radiation. If an incoming ray is incident on the trough at a point $\mathbf{P_i} = (x_i,y_i,z_i)$, then we desire to find the point $\mathbf{P_r} = (x_r,y_r,z_r)$ at which the reflected ray strikes a planar receiver placed at $z = f$, where f is the focal length of the trough. Rather than deriving $\mathbf{P_r}$ using the vector law of reflection, a much simplified analysis is possible if we use as a starting point the property of a parabolic trough that any plane of parallel incident rays, oriented as described above, will all be focussed to a single point, which is always at $z = f$ above the vertex of the trough. This implies that we have $x_r = 0$, $z_r = f$, and it only remains to determine y_r.

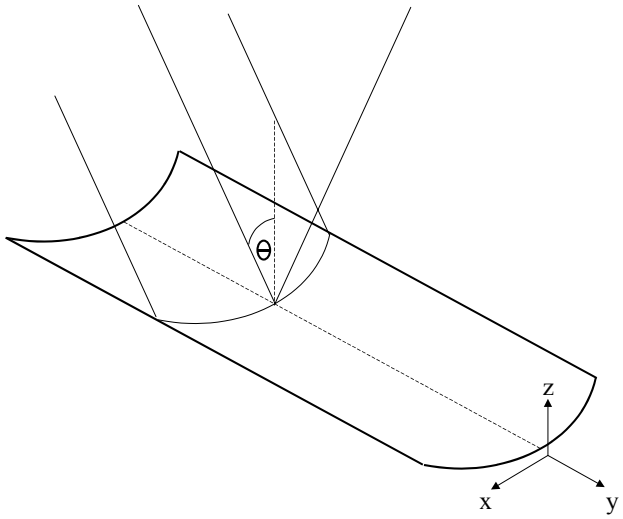

Figure 1 Trough geometry with incident plane of rays

The general equation of a plane can be written ax + by + cz = d, where (a,b,c) defines a normal to the plane. We are interested in a plane which represents the xz plane rotated about the x axis, the normal to which will have no x component, i.e. a=0. For simplicity we can also set that the plane passes through the origin, giving d=0 and reducing the equation of the plane to by + cz = 0. If θ is the angle between the plane and the z axis (see Figure 1) then we can write the equation of the plane as

$$y = -z\tan\theta \tag{1}$$

The parabolic trough is defined by

$$z = x^2/4f \tag{2}$$

and then combining (1) and (2) gives the line of incidence on the trough as

$$y_i = -\left(x_i^2/4f\right)\tan\theta \tag{3}$$

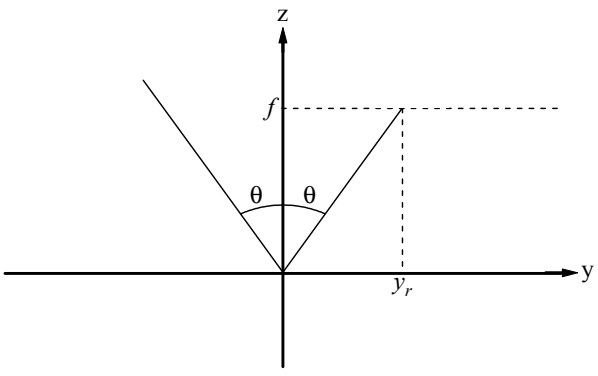

Figure 2 Reflection of central ray

To determine the point of intersection y_r at the receiver, consider the ray which strikes the trough at the vertex, $x_i = 0$. At that point the mirror normal is parallel to the z axis so there is no x direction change and Figure 2 shows the reflection to the focal plane. The ray is reflected along the y axis by an amount

$$y_r = f \tan\theta \tag{4}$$

and then from (3) and (4), the translation along the y axis is given by

$$y_r - y_i = \left(f + \frac{x_i^2}{4f} \right) \tan\theta \tag{5}$$

We can rewrite (5) as

$$y_i = \left(y_r - f \tan\theta \right) - \frac{x_i^2}{4f} \tan\theta \tag{6}$$

where it is seen that the source line for a point at the receiver is an inverted parabola in the xy plane.

3. GAPS IN THE REFLECTIVE SURFACE

Gaps in the reflective surface, along the length of a complete trough, produce non-uniformity in the flux distribution at the receiver. Consider that there is a series of photovoltaic cells at the receiver, each of length c. Define also that there are one or more gaps which go across the reflective surface, each of length g. We seek to determine the maximum loss of energy at a cell.

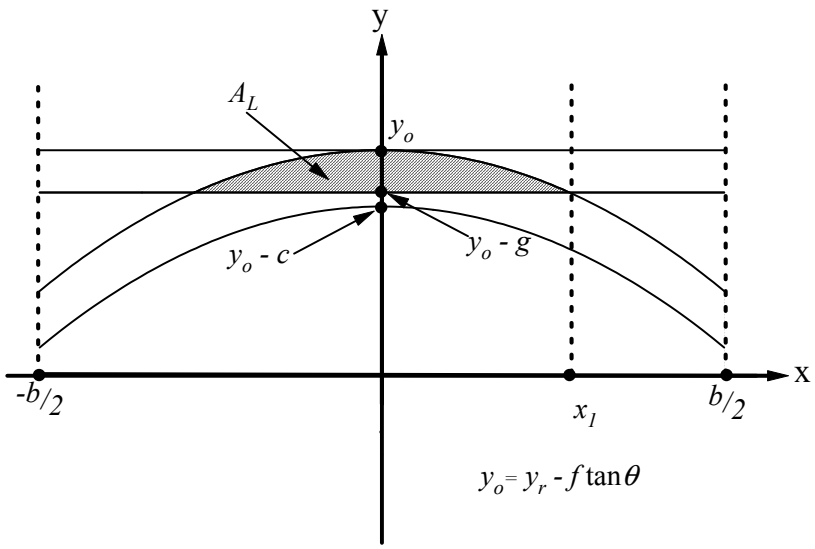

Figure 3 Intersection of flux source region and mirror gap

Equation (6) specifies the curve in the xy plane, on the trough, where incident light must fall to be reflected to the receiver at y_r. The total flux which falls on a cell which extends between y_r and $y_r + c$ is then proportional to the area between two parabolic curves separated by c (see Figure 3). The maximum loss of flux due to a gap will occur when the intersection area of the gap and the source region is maximized. In Figure 3 the highest points of the flux source area and the gap have been made coincident, so as to maximize the intersection area. The problem then becomes that of determining the shaded loss area A_L, compared to the total potential source area A_T. Note that Figure 3 shows one particular case, with g<c, and where the lower intersection point x_1 between the lower curve and the upper limit of the gap band is less than b/2, where b is the aperture of the mirror. In all there will be four cases to consider, being the combinations of g less or greater than c, and x_1 less or greater than b/2. Note that the value of x_1 depends on θ, as tan θ appears in the equation for the curve, and θ in turn depends on the season and time of day. For the usual situation of g<c then equations (7)-(10) apply.

$$x_1 = 2\left(\frac{fg}{\tan\theta}\right)^{1/2} \tag{7}$$

$$A_L = \frac{8g}{3}\left(\frac{fg}{\tan\theta}\right)^{1/2} \qquad \text{for } x_1 \le b/2 \tag{8}$$

$$A_L = bg - \frac{b^3 \tan\theta}{48 f} \qquad \text{for } x_1 \ge b/2 \tag{9}$$

$$A_T = bc \tag{10}$$

For a particular geometry, defined by f, g and c, and an insolation angle θ, the maximum fractional loss of flux A_L/A_T can then be calculated.

3.1. Flux Loss Due to Mirror Limit

If the parabolic band which defines the source region for flux on a cell extends beyond the far end of the trough, then there will be a reduction of flux received at that cell, compared to a cell well away from the end. This is shown in Figure 4, where the 'gap' is now thought of as extending from y_L, the mirror limit, to negative infinity.

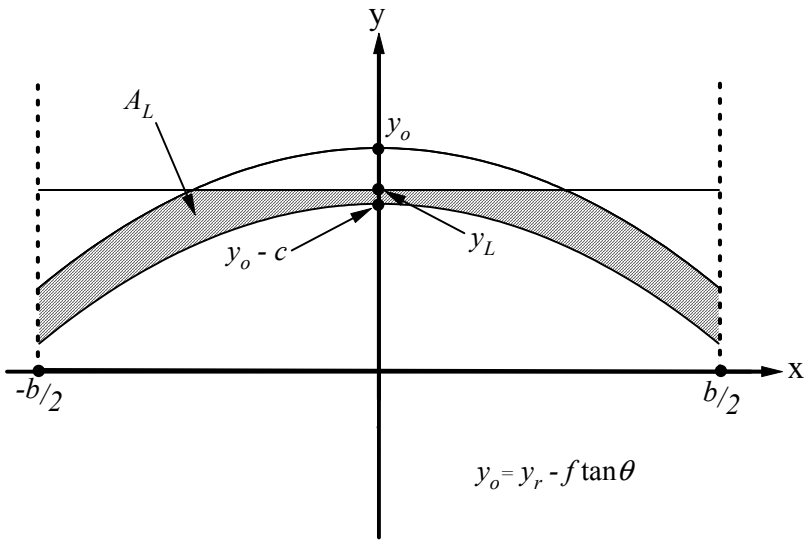

Figure 4 Flux loss due to mirror limit

The flux loss will again be proportional to the area A_L. Qualitatively, at the end of the flux line in the direction of the sun (for other than normal incidence), there will be an increase in intensity from zero up to the maximum value captured on a cell.

3.2. Lengthening of the Flux Line

Equations (8) and (9) overestimate the loss of flux due to a mirror gap, as imperfections in the mirror shape, as a number of factors may contribute to a lengthening of the flux line, relative to mirror length. These include:

- the angular width of the sun
- any convexity along the y axis of the trough resulting from the manufacturing process
- if the parabolic shape is produced by elastically deforming an initially flat (or nearly flat) surface, then a small anticlastic curvature will tend to be produced across the other dimension
- localized mirror or shape imperfections

Figure 5 Parabolic trough module

In order to determine the contribution of trough shape, coarse mesh photogrammetry was carried out on a Glass-On-Metal-Laminate parabolic trough module, constructed at the Centre for Sustainable Energy Systems (see Figure 5). The trough had focal length 700mm, aperture 1260mm, and length 1600mm. Five rows, each of 10 retroreflective targets were placed along the trough, at varying distances x from the axis of the trough. A series of 24 digital images were taken from different angles, using a Kodak DCS420 digital camera, and subsequently processed using Visual Measurement System (VMS) software. Post-processing was carried out using software written in Interactive Data Language (IDL). The xyz coordinates of the target points, as determined by the photogrammetry, were compared to an ideal trough as defined by equation (2). Figure 6 shows the resulting dz values, where $dz = z_{actual} - z_{ideal}$.

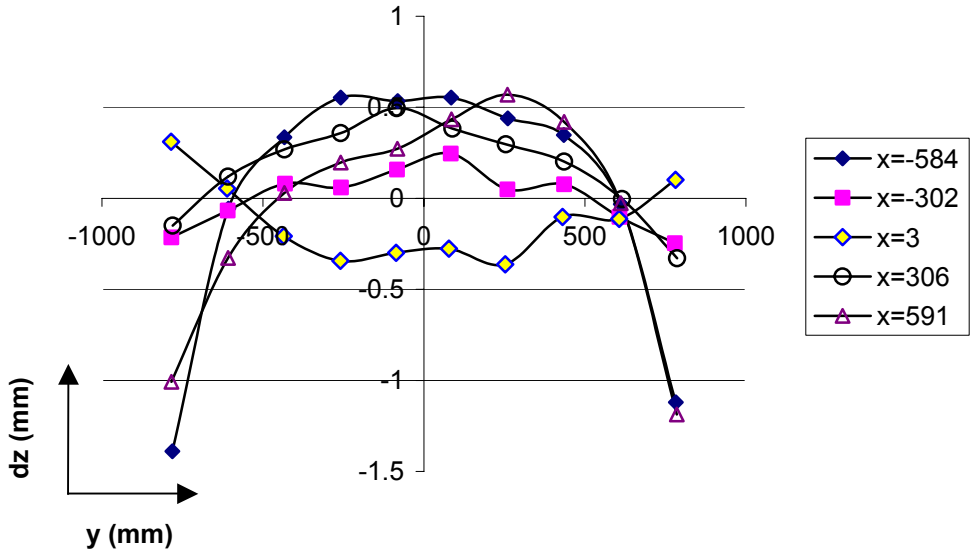

Figure 6 Trough height deviation from ideal (trough z axis horizontal)

Figure 6 shows the results for photogrammetry carried out with the trough z axis horizontal, which minimizes the gravitational sag of the mirror. The photogrammetry was repeated with z axis vertical, with no significant difference to the results: the mean difference between the $dz_{horizontal}$ and $dz_{vertical}$ values was 0.085mm, comparable to the mean precision of the xyz observations, at 0.05mm.

Whilst a much finer mesh would be required for accurate ray tracing, an estimate of the magnitude of the flux lengthening can be made using the existing photogrammetric data. In Figure 6, the outer lines (x=-584mm, x=591mm), are seen to have the greatest convexity. Their mean slope dz/y near the edges of the trough (y limits) is 0.0076, or a slope error of 7.6mrad. If L is the distance between the point of incidence on the mirror and the point at which the reflected ray strikes the target, and ε is the mirror slope error (assumed small) then the deviation Δy of the ray along the y axis is given by 2εL. Allowing also for a solar half angle α then

$$\Delta y = (2\varepsilon + \alpha)L \tag{11}$$

In the special case of θ=0º orientation, L is given by

$$L = f + z = f + \frac{x^2}{4f} \qquad \text{for } \theta = 0 \tag{12}$$

Combining (11) and (12)

$$\Delta y = (2\varepsilon + \alpha)\left(f + \frac{x^2}{4f}\right) \qquad \text{for } \theta = 0 \tag{13}$$

It is evident that the largest Δy occurs for the maximum value of x: substituting f=700, x_{max}=630, α=.00465, ε_{max}=0.0076, gives Δy_{max}=16.7mm, for incident rays parallel to the trough z axis. As rays incident nearer the vertex are deflected a lesser amount, a tapering off of the flux intensity would be expected.

4. FLUX MAPPING

Two trough modules with focal length = 700mm, arc length = 1300mm, aperture across the curve = 1260mm were placed end to end, such that there was a variable gap between their mirror surfaces. Images of the flux on a uniform white target placed at the focal plane were captured using a Kodak Megaplus ES1.0 video camera, for a variety of different insolation angles, for two different gap sizes. Note that one trough was not well adjusted for the set focal length and produced a split flux line. Figure 7 shows images taken with a 25mm mirror gap.

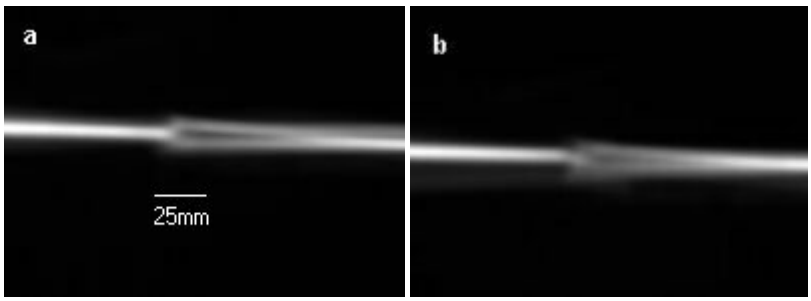

Figure 7 Flux images for 25mm gap, 0˚ (a) and 10˚ (b) orientations.

The most significant feature of Figure 7 is that there is no observable gap in the flux, despite the 25mm gap between the mirrors. This is in agreement with section 3.2, where for θ=0º orientation it was estimated that the flux line above the edge of a single mirror tapers off to a maximum lengthening of Δy=16.7mm. This will occur for the mirrors on both sides of the gap, so that the individual flux lines meet.

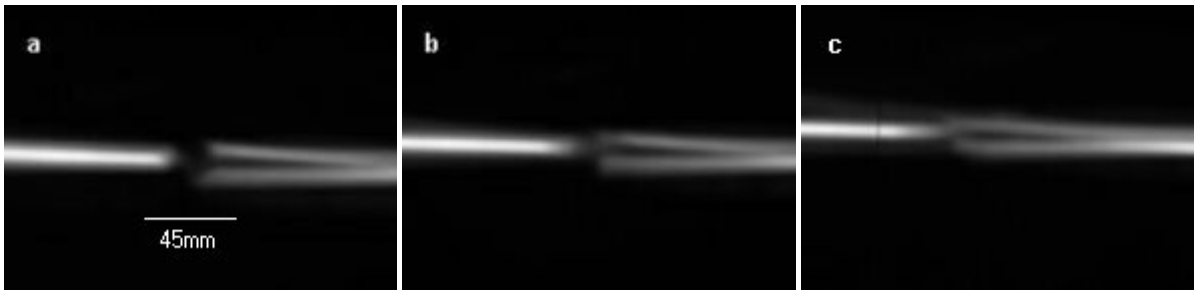

Figure 8 Flux images for 45mm gap: 0˚ (a), 11˚ (b), and 23˚ (c) orientations.

The flux images of Figure 8 were taken for an increased mirror gap of 45mm. In this case the lengthening is no longer sufficient to always close the gap between the flux lines of the two mirrors. In the case of 0º orientation there is a flux gap of approximately 21mm, which reduces to 15mm for 11º, and essentially disappears for 23º (the faint vertical black line in Figure 8c is an artefact of the processing of the camera images). As predicted by equations (8) and (9) the flux loss at the worst cell decreases as the orientation angle θ increases.

5. CONCLUSION

When a single-axis tracking trough is using with photovoltaic receivers, consideration must be given to the effect of non-uniformities in the flux distribution along the length of the array. Design of the complete system should allow for the reductions in received energy caused by mirror gaps and shadowing, so as to minimize or eliminate the time for which the loss of energy at any cell is sufficiently great so as to cause it to become reverse biased. Flux mapping and photogrammetry can be used in combination with theoretical analysis to assist in the design process.

ACKNOWLEDGMENTS

The assistance of Sawat Paitoonsurikan in preparing the figures is gratefully acknowledged.